Astron. Astrophys. 351, 945–953 (1999)

ASTRONOMY AND ASTROPHYSICS

New surveys of UBV photometry and absolute proper motions at intermediate latitude⋆

D.K. Ojha[1], **O. Bienaymé**[2], **V. Mohan**[3], **and A.C. Robin**[2,4]

[1] Tata Institute of Fundamental Research, Homi Bhabha Road, Colaba, Mumbai – 400 005, India
[2] Observatoire de Strasbourg, CNRS URA 1280, 11 rue de l'Université, 67000 Strasbourg, France
[3] Uttar Pradesh State Observatory, Manora Peak, Nainital, 263 129, India
[4] Observatoire de Besançon, 41 bis Av. de l'Observatoire, B.P. 1615, 25010 Besançon Cedex, France

Received 15 July 1997 / Accepted 29 September 1999

Abstract. A photometric and proper motion survey has been obtained in 2 directions at intermediate latitude: ($l = 167.5°$, $b = 47.4°$; $\alpha_{2000} = 9^h41^m26^s$,$\delta_{2000} = +49°53'27''$) and ($l = 278°$, $b = 47°$; $\alpha_{2000} = 11^h42^m56^s$, $\delta_{2000} = -12°31'42''$). The survey covers 7.13 and 20.84 square degrees, respectively. The limiting magnitude is about 18.5 in V for both directions.

We have derived the density laws for stars ($M_V \geq 3.5$) as a function of distance from the galactic plane. The density laws for stars follow a sum of two exponentials with scale heights of 240 pc (thin disk) and 790 pc (thick disk), respectively. The local density of thick disk is found to be 6.1±3% relative to the thin disk. The kinematical distribution of stars has been probed to distances up to 3.5 kpc above the galactic plane. New estimates of the parameters of velocity ellipsoid have been derived for the thick disk of the Galaxy. A comparison of our data sets with the Besançon model star count predictions has been performed, giving a good agreement in the magnitude range V = 13 to 18.

Key words: techniques: photometric – surveys – Galaxy: halo – Galaxy: kinematics and dynamics – Galaxy: stellar content – Galaxy: structure

1. Introduction

We have developed a programme of star counts on Schmidt plates in a few directions of the Galaxy. Objectives of this programme are to trace the fine structure of our Galaxy through the statistical study of the stellar distributions according to their luminosity, colors and proper motions. This involves two steps: first, acquiring a new photometric and astrometric sample survey in various galactic directions; and second analysing the data using a model of population synthesis and determining the properties of populations in the Galaxy and constraints on the scenario of formation and evolution. In the framework of this programme, new observations were carried out in selected areas situated in the main meridional section and towards galactic antirotation direction in the Galaxy. The combination of OCA, ESO, Tautenburg and Palomar Schmidt plates is used to derive the photometry and the absolute proper motions of the stars on a time baseline of about 35 years.

In our earlier work (Ojha et al. 1994ab; Robin et al. 1996), using the data from galactic anticentre and centre fields with wide-area surveys in other fields available to date, we discussed the radial and vertical structure of the Galaxy. By comparing the star count ratio between the two data sets (galactic anticentre and centre), we obtained the scale length of thin disk (h_R∼2.5 kpc) and thick disk populations (h_R∼3 kpc). The thick disk was found to have a scale height of 760±50 pc, with a local density of 5.6±1% of the thin disk. Our results confirmed no radial and vertical gradients in thick disk kinematics. The thick disk formation scenario was discussed based on the new photometric and kinematic data.

The present paper extends our previous work of a sample survey plan to produce probes of stellar populations in the Milky Way. The thick disk population is revisited under the light of new data. We have chosen a direction towards galactic anticentre at medium latitude ($l = 167.5°$, $b = 47.4°$; $\alpha_{2000} = 9^h41^m26^s$,$\delta_{2000} = +49°53'27''$; hereafter GAC2) and obtained BV star counts and absolute proper motion data in 7.13 square degrees for a complete sample of 6041 stars brighter than B = 20 mag. Schmidt plates from Tautenburg telescope were used to obtain magnitudes and color. Deep CCD sequences from 104-cm telescope of Uttar Pradesh State Observatory, Nainital (India) and 120-cm telescope from Observatoire de Haute-Provence (France) have been used to increase the magnitude limits up to V∼18.5 and B∼20. The choice of this particular area was made partly because this field gives the counterpart of the galactic centre field (Ojha et al. 1994b, hereafter GC, Paper II) and serves as a complement to the field toward the outer part of the Galaxy. The absolute proper motions of the stars in this field have been published elsewhere (Ojha et al. 1994a, hereafter GAC1, Paper I). Using the two fields (GAC1,2

Send offprint requests to: D.K. Ojha (ojha@tifr.res.in)

⋆ Based on observations made on photographic plates obtained with the Tautenburg, ESO and Palomar Schmidt telescopes and on CCD observations made at UPSO, Nainital (India) and OHP, France. Digitizations made with the MAMA measuring machine. MAMA is developed and operated by INSU (Institut National des Sciences de l'Univers, Paris).

Table 1. Plate material used for GAR field

Plate number	Emulsion + filter	Color	Epoch	Scale (”/mm)
Palomar Schmidt plates				
POSS 1562	103a-E+red plexiglass	red	10/03/1956	67.14
POSS 1562	103a-O+blue plexiglass	blue	10/03/1956	67.14
ESO Schmidt plates				
8520	IIaO+GG385	B	13/04/1990	67.13
8522	IIaO+GG385	B	15/04/1990	67.13
8551	103aD+GG495	V	18/05/1990	67.13
8557	103aD+GG495	V	19/05/1990	67.13
8556	IIaO+UG1	U	19/05/1990	67.13
8561	IIaO+UG1	U	20/05/1990	67.13
9172	IIaO+GG385	B	05/04/1991	67.13
9174	IIaO+GG385	B	06/04/1991	67.13
9193	IIIaF+RG630	R	12/04/1991	67.13
9194	IIIaF+RG630	R	12/04/1991	67.13
9246	103aD+GG495	V	05/05/1991	67.13
9254	IIIaF+RG630	R	05/05/1991	67.13

& GC) together is a good choice for sighting the intermediate population as shown in our preliminary studies (Paper I & II; Ojha et al. 1996 (hereafter Paper III); Robin et al. 1996).

The other survey is based on the measurement of 14 Palomar and ESO Schmidt plates covering an area of 20.84 square degrees centered on $\alpha_{2000} = 11^h42^m56^s$,$\delta_{2000} = -12°31'42''$ corresponding to $l = 278°$, $b = 47°$. This field is close to the galactic antirotation direction (hereafter GAR) at intermediate latitude. The catalogue contains about 22000 stars with completeness limits of V=18.5, B=20 and U=18.5. This field is a test direction to find evidence of the relative motions of the halo and intermediate populations. It also gives informations on the inclination of the velocity ellipsoids of these populations. These results will be published in future papers. A preliminary analysis of this catalogue together with a comparison with existing catalogues towards the same latitude (|b|) and with Besançon model of population synthesis is given elsewhere (Paper III & Robin et al. 1996). In the present paper, we discuss a new complete survey of absolute stellar proper motions and multicolor photometery. The more detailed analysis is also presented in the paper.

The outline of the paper is as follows: In Sect. 2, we discuss briefly the photographic plates used in the present surveys. The photographic calibration is explained in Sect. 3. In this section, we give the new color equations for the ESO and Tautenburg Schmidt plates. Sect. 4 describes the derivation of absolute proper motions and the overall accuracy of the proper motion surveys. In Sect. 5, we present the variation of the stellar number density as a function of distance from the galactic plane. From this, we deduce the structural parameters of the thin and thick disk population. In Sect. 6, we derive the kinematics of the thick disk component. Sect. 7 shows the comparison of our data sets with the Besançon model of population synthesis.

2. Photographic material

In the GAC2 field, among the 14 Schmidt plates used for the astrometric reduction described in Paper I (Table 1), we have chosen 2 Tautenburg Schmidt plates (2420 & 2430) in the V band (Kodak 103a-G+GG11) and 2 plates (6568 & 6569) in the B band (Astro-Spezial+GG13) for photometric purposes. Each plate covers an area of $3.°3\times3.°3$ with a scale of 51.4 arcsec mm^{-1}. All the plates were measured on the MAMA microdensitometer in Paris with a pixel size of 10 μm. The treatment of the plate with MAMA has been extensively described by Berger et al. (1991).

In the GAR field, 14 Schmidt plates from Palomar and ESO were used for the photometric and astrometric measurements. Plate descriptions are given in Table 1.

3. Photometric reduction

3.1. Photometric sequences

To photometrically calibrate the plates, a number of photometric standards are required. The standards should cover the entire range of magnitudes to be studied and should also be spread over the surface of the plate so as to minimise the geometrical effects present on the plate. To obtain the photometric standards, we have observed a number of subfields of each plate using the CCD system attached to the 1-metre telescope of the U. P. State Observatory at Nainital, India. A few standards have also been observed using the 1.2-metre telescope of Observatoire de Haute-Provence in France. The CCD images have been obtained in UBV filters. The image processing of the CCD images has been done using the ESO MIDAS and DAOPHOT softwares.

3.2. GAC2

Photographic BV magnitudes were derived from the total intensity using the BV photometric sequences for the present survey.

Table 2. Dispersion of magnitudes from plate to plate comparison in case of GAC2 field

V	σ_V	B	σ_B
11.75	0.02	11.25	0.02
12.75	0.03	12.25	0.02
13.75	0.03	12.75	0.03
14.25	0.04	13.25	0.03
14.75	0.04	13.75	0.02
15.25	0.04	14.25	0.03
15.75	0.04	14.75	0.02
16.25	0.05	15.25	0.03
16.75	0.05	15.75	0.02
17.25	0.05	16.25	0.03
17.75	0.05	16.75	0.03
18.25	0.06	17.25	0.03
		17.75	0.03
		18.25	0.04
		18.75	0.04
		19.25	0.05
		19.75	0.06

Table 3. Dispersion of magnitudes from plate to plate comparison in case of GAR field

V	σ_V	B	σ_B	U	σ_U
11.25	0.06	11.25	0.06	11.25	0.03
11.75	0.06	11.75	0.06	11.75	0.05
12.25	0.06	12.25	0.06	12.25	0.04
12.75	0.06	12.75	0.06	12.75	0.04
13.25	0.07	13.25	0.07	13.25	0.04
13.75	0.06	13.75	0.06	13.75	0.04
14.25	0.07	14.25	0.06	14.25	0.05
14.75	0.07	14.75	0.06	14.75	0.05
15.25	0.07	15.25	0.06	15.25	0.05
15.75	0.08	15.75	0.06	15.75	0.05
16.25	0.08	16.25	0.07	16.25	0.06
16.75	0.09	16.75	0.07	16.75	0.06
17.25	0.09	17.25	0.07	17.25	0.07
17.75	0.10	17.75	0.08	17.75	0.08
18.25	0.12	18.25	0.09	18.25	0.09
		18.75	0.09	18.75	0.10
		19.25	0.10		

The CCD magnitude sequences for this field were observed by Mohan et al. (1994) in the U, B, and V passbands. The BV photometric sequences include 110 stars for 11<V<21. A fourth-order polynomial function is fitted to these data to give the calibration curve for each plate. The rms scatters of the fitting are in a range of 0.02 to 0.06 magnitude in the V and B bands. The color equations to convert the instrumental system to the Johnson one have been derived by the procedures described by Mohan & Crézé (1987) and Ojha (1994). The following new color equations are derived for the Tautenburg Schmidt plates:

$$v_{inst} = V_{John} + 0.117(B-V) \quad (1)$$

$$b_{inst} = B_{John} + 0.113(B-V) \quad (2)$$

The plate to plate dispersion in all magnitude ranges is shown in Table 2.

3.3. GAR

Photometry is made using at least two plates per color in the three photometric bands UBV. Photometric sequences used are CCD photometric ones by Mohan et al. (1996). About 135 stars are typically used to determine the calibration curve in each passband. New color transformations between the Johnson system and the instrumental system of ESO Schmidt plates have been determined. The color equations are given as follows:

$$v_{inst} = V_{Johnson} - 0.130(B-V) \quad (3)$$

$$b_{inst} = B_{Johnson} - 0.143(B-V) \quad (4)$$

$$u_{inst} = U_{Johnson} + 0.245(B-V) - 0.056(U-B) \quad (5)$$

The typical rms magnitude scatter ranges from 0.03 to 0.12 in the magnitude range 11 to 19. The plate to plate dispersion in all magnitude ranges is shown in Table 3.

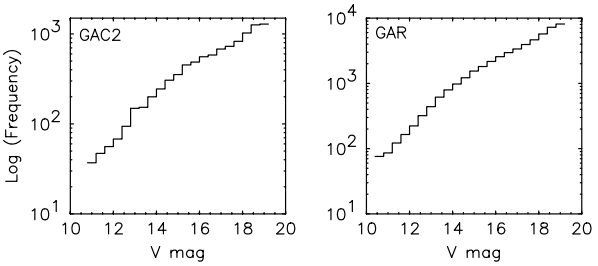

Fig. 1. Histograms of V star counts in GAC2 and GAR field. The completeness limit is V = 18.5

3.4. Star-galaxy separation

It is important to separate the galaxies from stars in the catalogue. The method of star/galaxy separation is described in our previous paper (Paper I). The classification of an image as a star or a galaxy was determined from the deepest and reference plate, V8557 in case of GAR field. Because the galaxy sequences merge with the stellar sequences at the faint end, this has the consequences that for V>18.5 the inclusion of galaxies in star bin is very high. For V$\leq$ 18, the discrimination between stars and galaxies is very good and there is essentially no contamination of the star counts by galaxies (see also Sect. 7). Similarly, Tautenburg plate 6568 was used to separate stellar and non-stellar objects in case of GAC2 field. The star-galaxy discrimination is reliable to V $\sim$ 18 mag.

3.5. Completeness

The instrumental photographic magnitudes are converted to the Johnson system using Eqs. (1) to (5). Histograms of standard V magnitude counts from GAC2 and GAR field are shown in Fig. 1. The completeness limits of the U, B and V counts are found to be 18.5, 20 and 18.5 in two fields.

Table 4. Starcounts over 7.13 square degrees as a function of V and B-V (GAC2 field)

B-V / V	-0.4	-0.2	0.0	0.2	0.4	0.6	0.8	1.0	1.2	1.4	1.6	1.8	2.0	2.2	Total
11.0–11.5	0	0	1	8	10	12	9	9	0	0	0	0	0	0	49
11.5–12.0	0	0	0	5	18	12	10	9	4	0	0	0	0	0	58
12.0–12.5	0	0	0	1	26	23	12	8	0	0	0	0	0	0	70
12.5–13.0	0	0	0	2	23	63	27	14	0	1	0	0	0	0	130
13.0–13.5	0	0	0	3	29	72	42	11	4	3	0	0	0	0	164
13.5–14.0	0	0	0	3	27	93	47	15	3	3	0	0	0	1	191
14.0–14.5	0	0	0	1	36	130	56	12	8	8	0	0	0	0	251
14.5–15.0	0	0	0	1	20	153	98	40	17	4	2	0	0	0	335
15.0–15.5	0	0	0	1	34	162	123	55	24	17	3	2	0	0	421
15.5–16.0	0	0	0	2	26	174	151	82	55	30	12	0	2	0	534
16.0–16.5	0	1	1	1	27	169	161	97	59	41	23	4	0	0	584
16.5–17.0	0	0	2	5	37	139	135	123	87	69	39	6	1	0	643
17.0–17.5	0	0	0	7	25	134	142	136	109	100	72	7	4	0	736
17.5–18.0	0	1	0	4	55	132	139	125	126	153	113	13	4	2	867
18.0–18.5	1	2	5	11	66	112	131	143	164	211	147	11	0	0	1004

Table 5. Starcounts over 20.84 square degrees as a function of V and B-V (GAR field)

B-V / V	-0.4	-0.2	0.0	0.2	0.4	0.6	0.8	1.0	1.2	1.4	1.6	1.8	2.0	2.2	Total
11.0–11.5	0	0	6	30	21	9	19	8	8	0	0	0	0	0	101
11.5–12.0	0	0	0	13	54	33	23	13	1	1	2	0	0	0	140
12.0–12.5	0	0	1	12	69	57	42	24	4	2	0	0	0	0	212
12.5–13.0	0	0	1	5	93	136	68	22	11	2	1	0	0	0	338
13.0–13.5	0	0	1	5	110	245	115	46	9	8	0	0	0	0	539
13.5–14.0	0	1	3	4	90	357	186	89	22	6	0	0	0	0	760
14.0–14.5	0	1	4	3	56	427	299	108	37	15	2	2	0	0	954
14.5–15.0	0	0	3	6	66	511	422	166	69	34	10	1	1	0	1289
15.0–15.5	0	1	3	5	83	580	547	221	83	59	25	1	3	0	1611
15.5–16.0	0	1	2	13	103	599	678	327	147	115	63	6	0	1	2056
16.0–16.5	0	2	12	17	143	690	686	374	182	139	107	21	3	0	2379
16.5–17.0	0	1	5	18	182	788	690	366	282	202	204	40	4	3	2786
17.0–17.5	1	2	12	34	303	843	708	427	277	298	296	68	7	0	3276
17.5–18.0	0	2	15	75	455	853	677	443	373	405	341	39	1	0	3677
18.0–18.5	2	7	32	128	616	964	714	494	273	105	0	0	0	0	3337

3.6. Photometric catalogues

Our final photometric catalogues include 6041 stars over 7.13 square degrees with BV magnitude and proper motions in GAC2 field and 22000 stars over 20.84 square degrees with UBV magnitude and proper motions in GAR field, respectively. Since both fields are at intermediate latitudes (|b|=47°), therefore the interstellar reddening is negligible, hence no correction has been applied to unreddened the main sequence. The observed starcount data are also presented in a tabular form in Tables 4, 5 and 6 for N(V,B-V) and N(V,U-B). The color-color diagrams of the sources from two fields are shown in Fig. 2. The full line shown in the figures locates the main sequence.

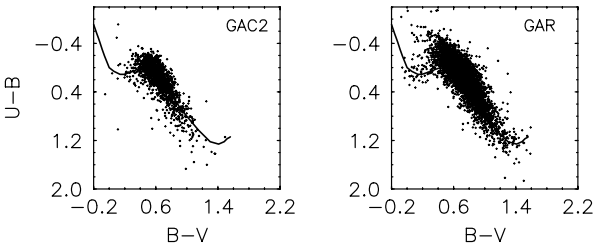

Fig. 2. U-B *versus* B-V diagrams of stars in GAC2 and GAR field. The full line locates the main sequence

4. Astrometry

For the astrometric reduction, the displacement of each stellar image is measured relative to the framework defined by all stars in the field. Then the relative proper motions have been shifted to absolute proper motions using the extragalactic objects in the field. Orthogonal functions were used to model transform between the plate coordinates. The distribution of reference stars is used to define an orthogonal system. This method is described in Bienaymé (1993) and in Paper I & II.

Table 6. Starcounts over 20.84 square degrees as a function of V and U-B (GAR field)

U-B / V	-1.0	-0.8	-0.6	-0.4	-0.2	0.0	0.2	0.4	0.6	0.8	1.0	1.2	1.4	1.6	1.8	2.0	2.2	Total
11.0–11.5	0	0	5	10	17	8	6	7	8	5	1	2	3	2	0	0	0	74
11.5–12.0	0	2	13	30	28	10	15	5	9	7	3	1	0	1	1	0	0	125
12.0–12.5	0	4	18	37	45	20	16	15	13	16	4	5	1	0	1	0	0	195
12.5–13.0	0	0	27	58	77	46	27	27	16	8	11	4	1	4	1	0	0	307
13.0–13.5	0	0	23	105	116	96	53	39	29	20	9	4	1	1	0	0	0	496
13.5–14.0	0	0	13	99	160	150	93	75	46	38	20	7	3	0	0	0	0	704
14.0–14.5	0	0	4	68	167	216	157	114	70	38	34	21	4	3	0	0	0	896
14.5–15.0	0	1	1	42	220	317	210	160	101	47	50	51	12	0	0	1	0	1213
15.0–15.5	0	0	1	33	207	376	296	209	137	101	63	58	7	0	1	0	0	1489
15.5–16.0	1	0	0	18	181	445	366	291	191	121	77	9	0	0	0	0	0	1700
16.0–16.5	0	2	1	18	240	522	404	277	187	62	5	0	0	0	0	0	0	1718
16.5–17.0	1	2	2	15	246	649	437	155	20	0	0	0	0	0	0	0	0	1527
17.0–17.5	0	1	3	18	335	533	135	1	0	0	0	0	0	0	0	0	0	1026
17.5–18.0	1	6	6	36	174	48	3	0	0	0	0	0	0	0	0	0	0	274
18.0–18.5	7	5	15	4	1	0	0	0	0	0	0	0	0	0	0	0	0	32

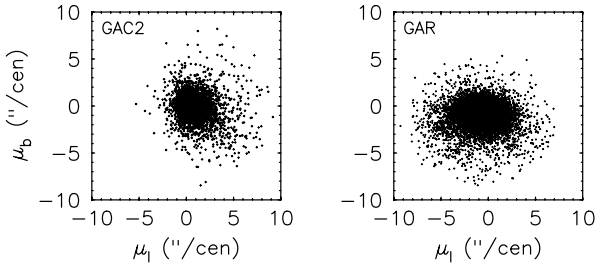

Fig. 3. Vector point diagram in GAC2 and GAR field

Table 7. The mean error (arcsec per century) in proper motion $< \sigma_\mu > = \sqrt{\sigma^2_{\mu_x} + \sigma^2_{\mu_y}}$ as a function of V magnitude in case of GAR field

V mag interval	$<\sigma_\mu>$ (”/cen)
11.25	0.22
11.75	0.22
12.25	0.23
12.75	0.22
13.25	0.21
13.75	0.19
14.25	0.20
14.75	0.18
15.25	0.14
15.75	0.15
16.25	0.12
16.75	0.12
17.25	0.12
17.75	0.13
18.25	0.17

4.1. Absolute proper motions

For GAR field, the mean proper motions of a sample of $\sim$ 3842 galaxies uniformly distributed in color (B-V<2.5) and magnitude ranges (12.5<V<18.5) has been used to calculate the zero point of the proper motions. The conversion equations obtained are as follows:

$$\mu_\alpha(abs) = \mu_\alpha - 0.65 \pm 0.02\ (''/\text{cen})$$
$$\mu_\delta(abs) = \mu_\delta - 0.27 \pm 0.01\ (''/\text{cen})$$

The mean error of the differential proper motions in arcsec per century as a function of V magnitude is given in Table 7.

The zero points of the proper motions for GAC2 field are given elsewhere (Paper I). In Fig. 3, the Vector Point Diagrams of the sources in two fields are presented. The asymmetric distribution in figures is consequence of the stellar asymmetric drift because of the growing contribution from higher velocity stars.

5. Space density of stars in GAR direction

5.1. Stellar distance

We have used BV photographic photometry to derive the distances of the sub-sample of stars. The distances were determined by estimating absolute stellar magnitudes, which were obtained from a M_V $versus$ B-V relation, taking into account the metallicity change as a function of the distance from the galactic plane. The derivation of the stellar distance estimates is explained in Paper III. We assume a vertical gradient of metallicity (∂ [Fe/H]/∂z = -0.3 kpc^{-1}) to correct the absolute magnitude (Kuijken & Gilmore 1989).

5.2. Density laws

We have derived the logarithmic space density functions of the thin and thick disk stars in 3.5$\leq M_V \leq$4.5 and 4.5$\leq M_V \leq$6.0 absolute magnitude intervals. The derivation for the space density of stars is explained in detail in Paper III. The observed density is fitted by the sum of two exponentials of the form shown in Eq. (1) in Paper III. The values of the scale lengths of thin

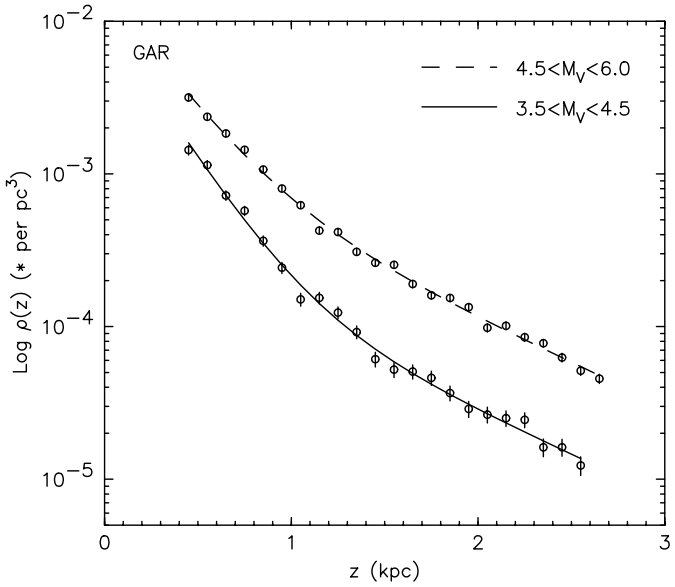

Fig. 4. The density distribution for stars with $M_V \geq 3.5$ as a function of distance above the galactic plane. The fitted lines represent the sum of two exponentials with scale heights given in Table 8

Table 8. The best fitted structural parameters of the thin and thick disk stars with $M_V \geq 3.5$ derived from the GAR field. The mean structural parameters derived from galactic anticentre and centre fields are also presented in the table

Field	Thin Disk	Thick Disk	Thin Disk: Thick Disk
$3.5 \leq M_V \leq 6$	h_z (pc)	h_z (pc)	density ratio
GAR	240±20	790±10	100: 6.1±3.0
GAC1,2	301±35	828±21	100: 8.0±0.7
GC	222±4	700±24	100: 9.8±0.1

and thick disk populations determined from the star count ratio (Paper III) were fixed in the calaculation.

A least-squares method is adopted to derive the best model in which the exponential distributions of the number density reproduce the observed starcounts. In Fig. 4, we present the density distribution of stars for two different absolute magnitude ranges, as a function of distance above the galactic plane. Table 8 presents the best fitted structural parameters for stars with $M_V \geq 3.5$ in GAR field. In the same table, we have also presented the mean structural parameters from the other two intermediate latitude fields (galactic anticentre & centre), which give an idea of the error on the determination.

The value of thin disk scale height ($h_z \sim 240$ pc) derived from GAR field is in agreement with the values obtained by Kuijken & Gilmore (1989) from a K dwarf photometric parallax study in the direction of the South Galactic Pole. Ng et al. (1995) determination gives h_z = 250 pc based on a sample of stars towards the galactic centre. Haywood (1994) and Haywood et al. (1997) showed that the overall vertical density profile of the galactic disk is closed to an exponential with scale height $h_z \simeq 250$ pc.

Our value of thick disk scale height derived from GAR field is in good agreement with the one derived from two intermediate latitude fields at galactic centre and anticentre (Paper III & Table 8). Robin et al. (1996) determination gives h_z = 760±50 pc, with a local density of 5.6±1% relative to the thin disk, which uses several fields to analyse the data using a synthetic model. Recently, Buser et al. (1999) find the Galactic thick disk to have local density of 5.9±3% of the local thin disk density and exponential scale height of h_z = 910±300 pc, using the new Basel RGU high-latitude survey.

6. Kinematics of thick disk population

The cardinal components of the stellar space velocity (in km s^{-1}), U, V and W were derived from proper motions, μ_l and μ_b (in arcsec year^{-1}) and distance d (in pc). In the direction of GAR field, we are measuring the velocities (U, V-W) defined as (see more detail in Paper III):

$$U \simeq 4.74\ d\ \mu_l cosb \quad \text{and} \quad \frac{V-W}{\sqrt{2}} \simeq 4.74\ d\ \mu_b$$

and we define:

$$\sigma^2_{V,W} = \frac{\sigma^2_V + \sigma^2_W}{2}\ .$$

To perform the kinematical separation in our sub-sample of stars (0.3<B-V<0.9), we have used a maximum likelihood method (SEM algorithm: Celeux & Diebolt 1986) in order to deconvolve the multivariate gaussian distributions and estimate the corresponding parameters. The aim of the SEM algorithm is to resolve the finite mixture density estimation problem under the maximum likelihood approach using a probabilistic teacher step. This method has already been used by Soubiran (1993ab) and in Paper I, II & III to characterize the (U,V,W) parameters of the stellar populations.

The samples of stars in GAR field have been devided in several bins of distance, and in each bin of distance, a fit has been performed with a SEM algorithm to separate the 2-D gaussian distributions to identify the three components (thin disk, thick disk and halo) of the Galaxy. In Fig. 5, the three gaussian populations representing the thin disk, the thick disk and the halo are overplotted on the (V-W)/$\sqrt{2}$ velocity histogram for the distance interval 1000≤d≤1500 pc. The mean kinematic parameters of thick disk derived from GAR field, up to the distance of 3.5 kpc above the galactic plane is shown in Table 9. In the same table, we have also presented the kinematics of the thick disk population obtained from the galactic anticentre and centre fields.

The thick disk parameters derived from GAR field are in good agreement with others: Soubiran 1993ab; Beers & Larsen 1995; Bartasiute 1994 and Paper III (derived from 2 intermediate latitude fields). By combining the four fields, GAC1,2, GC, GAR and NGP (Soubiran 1993ab), we have derived the mean kinematical parameters of thick disk (as shown in Table 5 in Paper III), which are: σ_U = 67±4 km s^{-1}, σ_V = 51±3 km s^{-1}, σ_W = 40 km s^{-1} and V_{Lag} = -53±10 km s^{-1} (with respect to the Sun). We do not find any evidence for a vertical gradient in

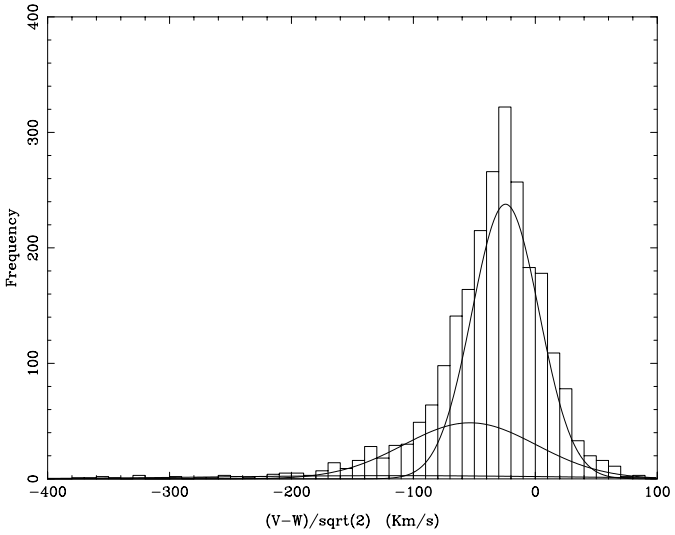

Fig. 5. Histogram of the $\frac{V-W}{\sqrt{2}}$ for stars in distance interval 1000≤d≤1500 pc towards GAR direction. The 3 gaussian components solution of SEM corresponding to thin disk, thick disk, and halo are overplotted

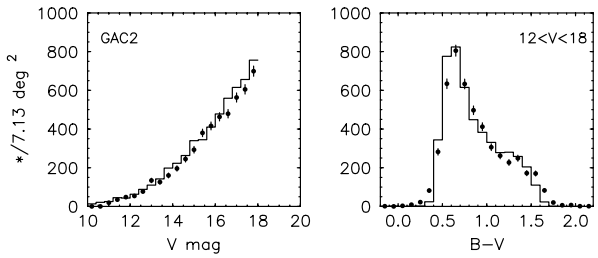

Fig. 6. Comparison of V star counts and B-V color between the observed data sets and the Besançon model predictions towards GAC2 direction. The histogram represents the model predictions. The filled circles are the observed data

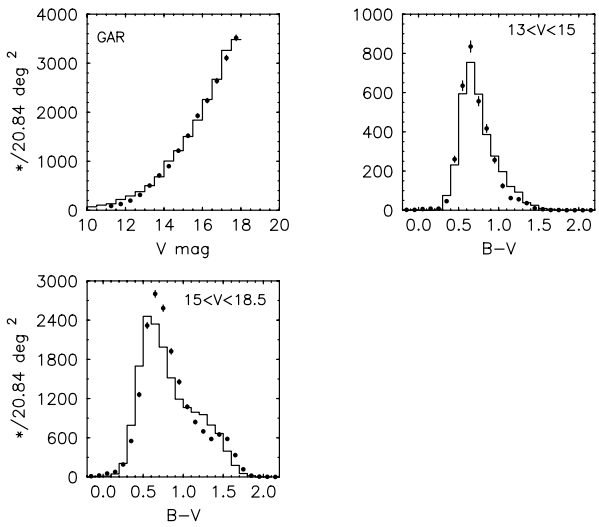

Fig. 7. Comparison between the observed V star counts & B-V color distributions and the model predictions towards GAR direction. The symbols are as in Fig. 6

Table 9. The mean kinematic parameters of thick disk (in km s^{-1}) derived from GAR field. The kinematic parameters derived from galactic anticentre and centre fields are also presented in the table

Antirotation (GAR)	Anticentre (GAC1,2)	Centre (GC)
σ_U = 67±12	$\sigma_{U,W}$ = 64±4	$\sigma_{U,W}$ = 66±3
$\sigma_{V,W}$ = 51±12	σ_V = 60±3	σ_V = 56±2
$\frac{<(V-W)>}{\sqrt{2}}$ = -49±10	$< V >$ = -57±4	$< V >$ = -49±3

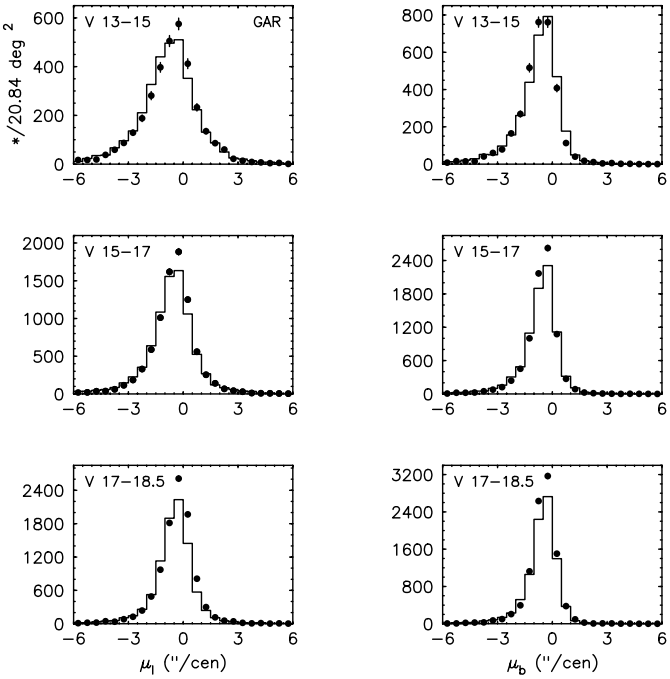

Fig. 8. Comparison of μ_l & μ_b distributions with the model predictions towards GAR direction. The symbols are as in Fig. 6

the thick disk kinematics in GAR field, in agreement with our previous results in the anticentre and centre fields, and with the field near the pole (Soubiran 1993ab). The suggested gradient from Majewski (1992) is not confirmed. As shown in Table 6 in Paper III that since 5–6 years, the accuracy of the kinematical measurements of the thick disk population has greatly improved and the results are well in agreement with each others.

7. Comparison of our data sets with Besançon model of stellar population synthesis

7.1. Besançon model

The data have been compared to the Besançon model (Robin & Crézé 1986, 1996; Bienaymé et al. 1987; Haywood 1994, 1997), by simulating the distributions of magnitudes, colors and proper motions including the photometric and astrometric errors as determined. The Besançon model of stellar population synthesis has been developed for about 13 years as an attempt to put together all constraints (theoretical and observational) about galactic evolution in order to obtain a consistent scenario of galaxy evolution. We used the new version of the

model (Robin et al. 1999). To minimize the Poisson noise in model simulations, the catalogues are simulated 5 or 10 times the total area of the observed data set. While the simulations in the two fields are qualitatively in agreement with the data, some discrepancies exist. In particular, the model overpredicts the number of stars in the GAC2 field beyond V>17 (Fig. 6). In GAR field, the number of stars are also slightly overpredicted at the bright magnitudes (V<12) (Fig. 7). All together, the models seem to predict slightly more red disk stars than visible in the data (B-V∼1.0–1.2). The comparison between the model predictions and the observed magnitude, color and proper motion distributions in two galactic fields is shown in Figs. 6, 7 & 8.

7.2. GAC2 field ($l = 167.5°$, $b = 47.4°$)

The distribution of the observed star counts in V band is shown in Fig. 6. In the same diagram, the model predicted counts are overplotted. The error bars are $\pm\sqrt{N}$, where N is the number of stars in each bin. The two distributions are in good agreement in the magnitude range 11<V<17, however, we find that the model predicts slightly more stars beyond V = 17 towards this direction. The possible reasons of this discrepancy between the model and data are discussed in Sect. 8.

The comparison between the observed data set and the Besançon model predictions in B-V color indice is also shown in Fig. 6. There is a good agreement between the two distributions in the magnitude range 12≤V≤18. At B-V ∼ 1.2 (in Fig. 6), the more red disk stars are seen in the model compared to the data.

7.3. GAR field ($l = 277°$, $b = 47°$)

Fig. 7 shows the observed V distribution towards GAR field. We compare these observations with the predictions of the Besançon model overplotted on the same figure. The total observed counts are in good agreement with the model predictions in the magnitude range 12<V<18, however, the contribution of blue stars at V<12 is slightly larger in the model.

The comparison between the observed distributions and the model predictions in B-V color indice is also shown in Fig. 7. The two distributions in B-V color are in good agreement in the magnitude range 13<V<15. In the magnitude range 15<V<18.5, the model overpredicts the red disk stars (B-V >1.0).

Model predicted proper motions distributions are compared to the observed ones in Fig. 8, assuming the same observational errors. The proper motion distributions (in μ_l & μ_b) agree well for stars in all the magnitude ranges. The mean velocity ellipsoid of the thick disk population used in the model simulation is the one deduced from our previous investigations in intermediate latitude fields and from the present paper. Due to the stellar drift, the asymmetric shape of the distribution of latitude proper motion is clearly visible in data and model. Proper motion distribution is sensitive to the asymmetric drift and the velocity dispersions of the stellar populations. The comparison between the data and model distributions in Fig. 8 is quite well, particularly at 15<V<17, where the majority of thick disk stars exist. It also proves that our value of the thick disk velocity ellipsoid is well determined.

7.4. Discussion

We have matched our data sets against the Besançon model of population synthesis. The main aim of these comparisons is to check the coherence of the model. Although, the total number counts brighter than V=18.5 are in relatively good agreement with observations, the contribution of blue stars of disk (V<12) is slightly larger in the model in GAR direction. The reason of this discrepancy is difficult to trace back with the present data. It could be attributed to two different parameters in the model, or a mixed of these two: the HR diagram (e.g the relative distribution of disk stars in the HR diagram) or the normalisation adopted for the disk stars, the 2nd parameters being the most critical. Since there is almost no data available to constraint the model between magnitudes 9–12, the model is almost entirely defined by its fit to the solar neighborhood luminosity function (See Haywood 1994, Haywood et al. 1997). The luminosity function (LF) adopted to normalize the model was that published by Wielen et al. (1983), and it is known to overestimate the number of stars in the 25 pc sphere by almost 30% (Turon, 1996). This problem could also be attributed to the distribution of the disk stars in the HR diagram, in particular, since the B-V color at bright magnitudes (V=9–12) are uncorrectly shifted to the red. However, simulations made with different SFR for disk stars, changing the relative distribution in the HR diagram, did not improve significantly the B-V model-data comparisons. One expects that these two aspects will be much better known now after the analysis of the Hipparcos and Tycho catalogues, which provides strong contraints on the distribution of the stars at V<10.5. Besançon model is in further improvement phase by using the data from Hipparcos and Tycho catalogues.

At fainter apparent magnitudes, where the disk becomes less important (V>12), the predictions are in good agreement in B-V (Figs. 6 & 7). At V>12, the absolute magnitude of the dominant stars is not the same that at V<12. However, at V=16–18, there are again slightly more stars in the model than in the data, in the two fields at B-V ∼ 1.2. This can not be attributed to incompletness in the data, since the catalogues are completed up to V=18.5 and B=20. According to galactic models, red stars (B-V>1) at these magnitudes (V>17) are disk stars, whereas at B-V≥1.2 and 16<V<17, there is a number of thick disk stars which could eventually make the overprediction of the model. This discrepancy could be due the luminosity function of the thick disk which may be inappropriate, if this is not the density law. If the present discrepancy is significant, one could possibly be attributed to unresolved binaries also, which are not accounted for in the model.

8. Conclusions

We have presented a new survey of absolute stellar proper motions and multicolor photometry to V = 18.5 in two directions at intermediate latitude. The most probable value of scale height

for the thick disk stars in GAR direction is determined to be $h_z \simeq 790 \pm 10$ pc with a local density of $6.1 \pm 3\%$ relative to the thin disk. The velocity ellipsoid of the thick disk component has been determined. These values are in perfect agreement with the recent determination given by Robin et al. (1996) and Ojha et al. (1996) based on the analysis of a large set of available photometric and astrometric catalogues. The Besançon model predictions are also compared with the present survey in the overlapping magnitude ranges.

Acknowledgements. This research was partially supported by the Indo-French Center for the Promotion of Advanced Research / Centre Franco-Indien Pour la Promotion de la Recherche Avancée, New Delhi (India). We thank all the MAMA, ESO, Tautenburg and Leiden Observatory staffs who made this investigation possible. We especially thank referee Dr. Gerry Gilmore for his comments. We also thank Misha Haywood for going through an earlier version of this manuscript and giving his useful comments. This research has made use of the DEC-ALPHA system of the Optical CCD astronomy programme of TIFR.

References

Bartasiute S., 1994, Baltic Astronomy vol. 3, p. 16
Beers T.C., Sommer-Larsen J., 1995, ApJS 96, 175
Berger J., Cordoni J.P., Fringant A.M., et al., 1991 A&AS 87, 389
Bienaymé O., Robin A.C., Crézé M., 1987, A&A 180, 94
Bienaymé O., 1993, A&A 278, 301
Buser R., Rong J., Karaali S., 1999, A&A 348, 98
Celeux G., Diebolt J., 1986, Rev. de Statistiques Appliquées 34, 35
Haywood M., 1994, A&A 282, 444
Haywood M., Robin A.C., Crézé M., 1997, A&A 320, 428
Kuijken K., Gilmore G., 1989, MNRAS 239, 605; 651
Majewski S.R., 1992, ApJS 78, 87
Mohan V., Crézé M., 1987, A&AS 68, 529
Mohan V., Ojha D.K., Bienaymé O., et al., 1994, Bull. Astron. Soc. India. 22, 403
Mohan V., Sanwal B.B., Paliwal D.C., et al., 1996, Bull. Astron. Soc. India 24, 7
Ng Y.K., Bertelli G., Bressan A., et al., 1995, A&A 295, 655
Ojha D.K., Bienaymé O., Robin A.C., Mohan V, 1994a, A&A 284, 810 (Paper I)
Ojha D.K., Bienaymé O., Robin A.C., Mohan V., 1994b, A&A 290, 771 (Paper II)
Ojha D.K., 1994, Ph.D. Thesis, Strasbourg University, France
Ojha D.K., Bienaymé O., Robin A.C., Crézé M., Mohan V., 1996, A&A 311, 456 (Paper III)
Robin A.C., Crézé M., 1986, A&A 157, 71
Robin A.C., Haywood M., Crézé M., Ojha D.K., Bienaymé O., 1996, A&A 305, 125
Robin A.C., et al., 1999 (in preparation)
Soubiran C., 1993a, A&A 274, 181
Soubiran C., 1993b, In: MacGillivray H.T. et al. (eds.) IAU Symp. NO. 161, Astronomy from wide field imaging. Potsdam, Germany, p. 435
Turon C., 1996, De l'utilisation des données Hipparcos. Atelier du GDR, CNRS, France
Wielen R., Jahreiss H., Kruger R., 1983, In: Philips D., Upgren A. (eds.) The Nearby Stars and the Stellar Luminosity Function. IAU Coll. 76